Interplay between Ising and six-vertex symmetries in a model for the roughening of reconstructing surfaces

1990 J. Phys. A: Math. Gen. 23 5625

(http://iopscience.iop.org/0305-4470/23/23/032)

J. Phys. A: Math. Gen. **23** (1990) 5625–5646. Printed in the UK

Interplay between Ising and six-vertex symmetries in a model for the roughening of reconstructing surfaces

J Kohanoff†‡, G Jug†§ and E Tosatti†||

† International School for Advanced Studies, Strada Costiera 11, 34014 Trieste, Italy

Received 11 April 1990

Abstract. We study a generalization of the solid-on-solid (SOS) model recently proposed for the roughening transition of reconstructing and non-reconstructing FCC [110] solid surfaces. The generalized model is expressed in terms of Ising variables representing nearest-neighbour atomic column height differences. The model is solved exactly for the order–disorder transition, obtained in the limit where all possible Ising configurations are allowed. In the opposite limit, where the local height conservation rule is imposed to recover the BCSOS (or six-vertex) symmetry, finite-size transfer-matrix calculations yield a phase diagram where the reconstruction transition (corresponding to the order–disorder transition in the other limit) is smeared out, and a roughening transition occurs at a higher temperature. The phase boundaries obtained in the two limits (Ising and BCSOS) are compared. The model Hamiltonian contains a single parameter (λ), which connects in a natural way these limiting cases ($\lambda = 0$ and ∞ respectively). We study by finite-size calculations a simplified version of this Hamiltonian, named the λ-model, which just interpolates between the simple Ising model and Rys's F-model. In particular, we analyse the behaviour of the correlation length and the heat capacity peak for the whole range of values of λ, and the step free energy for λ large enough. When the six-vertex constraint is gradually removed (by decreasing λ), the roughening temperature—still well defined near the BCSOS limit—is found to be almost constant down to a particular value of λ, followed by a very fast growth towards $T = \infty$ for $\lambda \to 0$.

1. Introduction

The theory of structural phase changes at the surface of crystalline bulk materials is an active area of research in statistical mechanics. Of particular interest is the roughening transition of a solid surface, which determines the type of crystal growth mechanism associated with the material in given thermodynamic conditions (van Beijeren and Nolden 1987). Nucleation of atomic steps, characterized by an energy barrier, dominates below the roughening temperature, whilst macroscopically the transition is associated with the disappearance of a specific crystal facet and the vanishing of the free energy for step formation.

Much studied, amongst many examples, are the [110] faces of FCC noble-metal single crystals, which are also characterized by the possibility of presenting a reconstructed low-temperature smooth phase with a different (1×2 missing-row) symmetry from that of the bulk crystal structure. There has been considerable theoretical

‡ Present address: IBM Zürich Research Division, 8803 Rüschlikon, Switzerland.

§ Theory and Computational Science Group, AFRC-IFRN, Colney Lane, Norwich NR4 7UA, UK.

|| International Centre for Theoretical Physics, Strada Costiera 11, 34014 Trieste, Italy.

0305-4470/90/235625+22$03.50

(Jayaprakash and Saam 1984, Trayanov *et al* 1989a, b) and experimental interest in the roughening of non-reconstructed FCC [110] noble-metal surfaces, particularly in the cases of Cu (Mochrie 1987, Zeppenfeld *et al* 1989), Ag (Held *et al* 1987) and Pb (Prince *et al* 1988, Yang *et al* 1989). Less effort has been devoted so far to the problem of roughening in 1×2 missing-row reconstructed noble-metal surfaces, e.g. Au (Campuzano *et al* 1985, Drube *et al* 1989), Ir (Hetterich and Heiland 1989) and Pt (Salmerón and Samorjai 1980, Robinson *et al* 1989), in particular to the question of whether the roughening transition coincides with or follows the order–disorder reconstruction transition normally studied in these systems.

Two other models have been proposed to date in order to provide a preliminary picture for the roughening of reconstructing surfaces. Villain and Vilfan (1988) have presented a statistics for the defect lines, and associated kinks, generated by thermal fluctuations within the 1×2 ground state configuration of Au [110]. Their analysis yields indications for two transitions, both Ising-like, one corresponding to the order–disorder reconstruction at T_c, the other to the roughening at T_R, and with $T_R - T_c \approx 100$ K in the specific case of Au. The second model, proposed by Levi and Touzani (1989), is stated in terms of an anisotropic and interacting six-vertex model which is solved numerically for the step free energy in order to establish the dependence of the roughening transition temperature on surface energy anisotropy. This model has the advantage of treating reconstructing and non-reconstructing surfaces on the same footing.

In this paper we study a modified version of a third model, proposed earlier by two of the present authors (Jug and Tosatti 1990a, b) in order to describe the dependence of both the roughening and deconstruction transition temperatures on surface energy anisotropy, as well as to elucidate the nature of the structural phases present between T_c and T_R. A preliminary analysis (Jug and Tosatti 1990a, b) of the model to be described later has shown that $T_R > T_c$, that roughening is of infinite-order (Kosterlitz–Thouless) whilst deconstruction is possibly Ising-like, and that between the two transitions a sequence of disordered incommensurate phases is present as precursor to true roughening. Here we present alternative results from a finite-size transfer-matrix study (Kohanoff 1989) indicating that this picture is essentially correct in predicting that $T_R > T_c$ for all reconstructing surfaces. A short version of this work has been presented elsewhere (Kohanoff *et al* 1990).

The theory contains a parameter κ—the so-called surface energy anisotropy—which measures the tendency towards missing-row 1×2 reconstruction. For $\kappa > 0$ the 1×2 reconstruction is more favourable than the unreconstructed ground state, while for $\kappa < 0$ the situation is reversed. We find that, while the roughening temperature T_R is relatively insensitive to the anisotropy κ, there is a deconstruction temperature T_c which falls to zero for $\kappa \to 0^+$, in order to rise again for $\kappa < 0$. We propose that our Hamiltonian in the regime $\kappa \leq 0$ provides a new description of the *dormant* FCC [110] surfaces. By that term we mean surfaces having only a weak tendency to reconstruct, usually requiring extra forces—like those provided by some adsorbates—in order to develop a 1×2 reconstructed ground state. Examples of dormant FCC [110] surfaces are Cu [110] and Ag [110] (Hayden *et al* 1983), and probably also Pd [110] and Ni [110]. Our results indicate that some kind of order–disorder transition should also be expected for such unreconstructed dormant surfaces. Moreover, the disordering temperature T_c is lower for a dormant surface which is closer to the reconstruction point $\kappa = 0$.

The model can be written in terms of two sets of column height variables, $\{h_{ij}\}$

and $\{l_{ij}\}$, each set being defined on the sublattice of one of the two inequivalent lattice layers (see figure 1(a)). Here we study a modified version of the model of Jug and Tosatti (1990), where the height differences $s_{ij,kl} = h_{ij} - l_{kl}$ between nearest-neighbour atomic columns at sites (i,j) and (k,l) are restricted to take the values ± 1 in units of the vertical interlayer lattice spacing. With such constraint (à la van Beijeren (1977)), our SOS Hamiltonian can be written in terms of Ising variables s_{ij} (now representing nearest-neighbour height jumps between the two sublattices) as:

$$\mathcal{H} = -\alpha \sum_{i \text{ even},j} s_{i,j}s_{i+1,j} - (\alpha - 2\beta) \sum_{i \text{ odd},j} s_{i,j}s_{i+1,j} - \sum_{i,j} s_{i,j}s_{i,j+1} + \mathcal{H}_{\square} \tag{1.1}$$

where the $\{i,j\}$ are now sites of the dual lattice of the combined $\{h\}\bigcup\{l\}$ lattice. At this point, it is important to notice that in the BCSOS system—representing a solid surface—not all spin configurations are allowed due to the local height conservation rule (ice-rule, or six-vertex constraint, see figure 1(b)):

$$s_{i,j} - s_{i+1,j} - s_{i,j+1} + s_{i+1,j+1} = 0 \tag{1.2}$$

$s_{i,j}$, $s_{i+1,j}$, $s_{i,j+1}$ and $s_{i+1,j+1}$ being the spins of each elementary lattice cell (broken squares in figure 1(a)). With such constraint enforced, the model has the symmetry of a six-vertex (BCSOS) model (Baxter 1982) and could indeed be rewritten in terms of two compenetrating but interacting six-vertex sublattices (Kohanoff 1989). However, no exact solution can be sought for this model, and we therefore resort (in section 3) to approximate treatments such as the finite-size scaling extrapolation of exact calculations on lattice strips (Barber 1983).

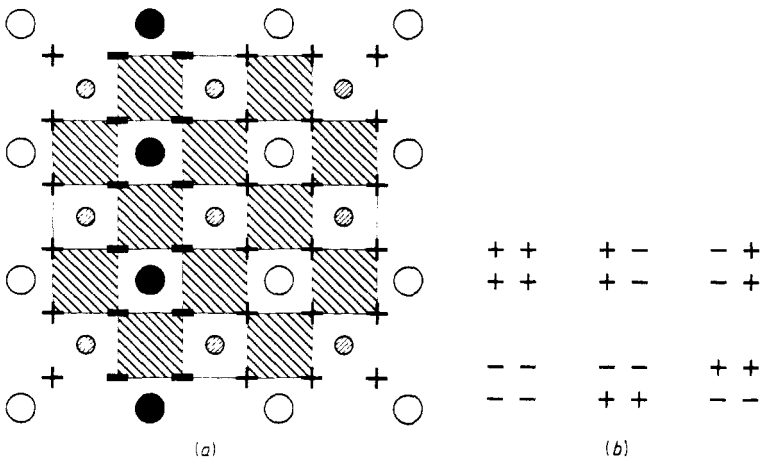

Figure 1. (a) Two-sublattice structure of the FCC [110] surface. Large circles indicate h-sublattice sites (empty circles at quote 0, full circles at quote -2), smaller circles l-sublattice sites (all at quote -1); for simplicity, both sublattices are taken as square. In this way, the left-hand side represents the ordered 1 x 2 structure, the right-hand side the 1 x 1 structure. + or − signs refer to nearest-neighbour height differences ('spins'). (b) Spin configurations allowed in each elementary plaquette, owing to local height conservation.

The last term $\mathcal{H}_{\square}$ in (1.1) is included in order to take into account this six-vertex constraint, and it is written

$$\mathcal{H}_{\square} = \lambda \sum_{\square} (s_{i,j} - s_{i+1,j} - s_{i,j+1} + s_{i+1,j+1})^2 \tag{1.3}$$

where the symbol '□' in the sum expresses that this term is included just for the broken squares (plaquettes) in figure 1(a). In this way we consider constraint (1.2), but in a wider context since it is achieved only in the limit $\lambda \to \infty$ in equation (1.3). Furthermore for $\lambda = 0$ an alternate-coupling Ising model is realized. In general, we have constructed a Hamiltonian able to connect continuously (by varying λ) an Ising-like model to another with the six-vertex symmetry.

Ground state considerations on Hamiltonian (1.1) (for any value of λ) show that the ferromagnetic + (or −) uniform spin configuration—corresponding to the non-reconstructed 1×1 $T = 0$ surface structure, for $\lambda \to \infty$—is favoured for $\kappa \equiv 4\beta - 2\alpha < 0$, whilst the modulated $\langle + - - + \rangle$ antiphase—representing the reconstructed 1×2 $T = 0$ surface structure, always for $\lambda \to \infty$—dominates for $\kappa > 0$. α is a parameter between 0 and 1 representing the lattice parameter anisotropy, so that in the following we shall work with square sublattices. Thus κJ, J being a measure of the atomic cohesion energy, can be loosely identified with the surface energy density anisotropy $\Delta = \sigma_{[110]} - \sqrt{\frac{3}{2}}\sigma_{[111]}$ between the [110] and [111] interface structures.

The aim of the present paper is to provide a quantitative determination of the main phase-transition temperatures in the model thus defined. In the six-vertex limit, at high temperatures, we expect the surface to become rough, in the sense that the free energy for step formation f_s will vanish at a specific roughening temperature T_R. At a lower temperature and for $\kappa > 0$ an Ising-type transition should occur in correspondence with the appearance of long-ranged 1×2 surface ordering. As pointed out elsewhere, this transition should arise owing to the double-degeneracy of the 1×2 $\langle + - - + \rangle$ ground state in the model. In our case the energy of the $\langle + + - - \rangle$ and $\langle - - + + \rangle$ uniform configurations is different from that of the $\langle + - - + \rangle$ and $\langle - + + - \rangle$ states. The latter are lowest in energy for $\kappa > 0$ and degenerate, so that at $T = 0$ there is indeed an Ising order parameter. Nonetheless this does not guarantee the existence of an Ising order–disorder transition at a finite T_c, as the true symmetry of the model is the six-vertex one, and not all possible thermally excited Ising configurations are allowed, owing to the constraint of local height conservation, equation (1.2). It is interesting to note that in the true physical 1×2 reconstructed systems, all four states are actually degenerate. In that case, the symmetry becomes that of the two-dimensional ANNNI model, were it not for the six-vertex constraint.

The situation for $\kappa < 0$ is, in principle, not symmetrical with respect to $\kappa > 0$. For $\kappa < 0$ there is no reconstruction, and the 1×1 surface can take only two $T = 0$ ordered configurations $\langle ++++ \rangle$ and $\langle ---- \rangle$. The former has $\{h\}$ as the uppermost sublattice, the latter has $\{l\}$. These two ground states are degenerate, and therefore give rise to an Ising order parameter as well. Again, considerations similar to those for $\kappa > 0$ can be applied to this case. There is in general room for an Ising transition at $T_c > 0$ whenever the six-vertex constraint is relaxed. Otherwise, we may expect disordering at $T \to 0$ when the six-vertex constraint holds.

The remainder of this paper is organized as follows. In section 2 we determine the phase boundary of the model by allowing all unrestricted Ising spin configurations, i.e. in the $\lambda = 0$ limit of (1.1). This immediately yields the order–disorder transition line, which we determine by solving exactly the alternate-coupling Ising model. In section 3 the phase boundaries for the physical, constrained Ising model (the $\lambda = \infty$ limit in (1.1)) are determined via finite-size transfer-matrix evaluations of the heat capacity and step free energy. Qualitatively there turns out to be no difference between the phase diagrams of the model in the two separate limits, Ising and six-vertex, as far as

is absent in the Ising limit, since the height variables become ill defined, whilst the spin variables still hold. Finally, in section 4 we consider a simplified version of the Hamiltonian (1.1), consisting of replacing the non-λ-dependent part, by the bare Ising Hamiltonian (isotropic, non-alternate), which we shall call the λ-model. Clearly the λ-model does not contain the original model, because it does not have alternating interactions (particularly for what concerns the sign of these interactions). However, it is simpler than (1.1), and very close in several aspects. By means of this Hamiltonian, we are able to study the continuous evolution (by varying λ) of the thermodynamic quantities, from the unconstrained to the constrained limit, i.e. to understand how the Ising-like critical behaviour merges into a Kosterlitz–Thouless-like behaviour for increasing λ. We also study the roughening transition in the region of small values of $\Lambda = \exp(-\lambda/T)$ (big values of λ), where the height jump is still a well defined quantity, at least on average. These results should carry on to a similar extension of the alternate-coupling Hamiltonian (1.1).

2. Phase diagram for the unconstrained Ising Hamiltonian: exact solution ($\lambda = 0$)

As pointed out in the introduction, it is of some interest to compare the phase diagram of the physical, constrained model—to be determined in the next section—with that of the same model where all Ising spin configurations are allowed on each elementary cell ('sixteen-vertex' model). The unrestricted Ising model for the surface structure has the important feature of being exactly solvable for the partition function, thus allowing for the possibility of testing our approximate transfer-matrix techniques for the determination of the model's properties. The exact solution should give at once the Ising order–disorder transition expected to be associated with reconstruction in a model with a doubly-degenerate ground state and Ising symmetry for the excitations. As an Ising model, Hamiltonian (1.1) in the limit $\lambda = 0$ belongs to the class of models with alternating nearest-neighbour spin couplings in both directions, the most general spin Hamiltonian being:

$$\mathcal{H}/T = -K_1 \sum_{i \text{ odd},j} s_{ij}s_{i+1j} - K_2 \sum_{i \text{ even},j} s_{ij}s_{i+1j} - K_3 \sum_{i,j \text{ odd}} s_{ij}s_{ij+1} - K_4 \sum_{i,j \text{ even}} s_{ij}s_{ij+1} \tag{2.1}$$

with $K_1, \ldots, K_4$ the four alternating coupling parameters. Since the lattice bond covering is not of the chequered type (i.e. the type that can be obtained by replacing the black squares of a chess-board with a single cell of bond strengths), we are not in the position here to exploit the general solution method outlined by Utiyama (1951). We know of no published method for the exact solution of Hamiltonian (2.1), and hence we outline our derivation based on a generalization of Vdovichenko's (1965) method for the solution of the Onsager problem†. In this procedure it can clearly be seen how to perform in practice the extension to other cases.

† After completion of this work, however, the formal solution for a problem containing the present model has been proposed by Holzer (1990).

The partition function is $\mathcal{Z} = \mathcal{Z}_0\mathcal{Z}_1$, with

$$\mathcal{Z}_0 = 2^N \left(\prod_{r=1}^{4} u_r \right)^{N/2} \tag{2.2}$$

$$\mathcal{Z}_1 = \frac{1}{2^N} \mathrm{Tr} \prod_{\langle ij,kl \rangle} (1 + t_{ij,kl} s_{ij} s_{kl}) \tag{2.3}$$

where in equation (2.3) the product is over all pairs of nearest-neighbour sites and where $u_r = \cosh(K_r)$, $t_{ij,kl} = \tanh(K_{ij,kl})$. The product can be evaluated via the usual high-temperature lattice graph expansion (Domb 1960)

$$\mathcal{Z}_1 = \sum_{L=0}^{2N} \sum_{l_1+\cdots+l_4=L} t_1^{l_1} \cdots t_4^{l_4} g_N(l_1, \ldots, l_4) \tag{2.4}$$

where $t_r = \tanh(K_r)$ and $g_N(l_1, \ldots, l_4)$ is the number of allowed graphs containing l_r bonds of strength t_r, $r = 1, \ldots, 4$. By extending the sum to all graphs with intersections and weighting each site in a graph with a phase factor $e^{i\phi_{ij}/2}$, ϕ_{ij} being the change in orientation of the vector tangent to the graph at site ij, we arrive at

$$\mathcal{Z}_1 = \sum_{L=0}^{2N} \sum_{s=0}^{\infty} \frac{(-1)^s}{s!} \sum_{L_1+\cdots+L_s=L} f_N(L_1) \cdots f_N(L_s). \tag{2.5}$$

Here, $f_N(L)$ is the contribution to $\mathcal{Z}_1$ from all weighted single-loop configurations of L bonds:

$$f_N(L) = \sum_{\text{Loops}} \sum_{l_1+\cdots+l_4=L} t_1^{l_1} \cdots t_4^{l_4} \prod_{ij \in \text{Loop}} e^{i\phi_{ij}/2}. \tag{2.6}$$

In order to evaluate $f_N(L)$ we reduce the problem to that of a random walk lattice path, weighted and oriented. Let us assign an index $a = 1, \ldots, 4$ to each orientation of a lattice site: 1 = right, 2 = up, 3 = left and 4 = down, and introduce the quantity $W_L^{aa',\alpha\alpha'}(\boldsymbol{x}, \boldsymbol{x}')$ as the sum over all weighted path configurations of L bonds between lattice sites $\boldsymbol{x}$ and $\boldsymbol{x}'$, starting at $\boldsymbol{x}$ with orientation a and ending at $\boldsymbol{x}'$ with orientation a'. The indices α and α' refer to the sublattices to which the sites $\boldsymbol{x}$ and $\boldsymbol{x}'$ belong, each sublattice now including all those sites with the same nearest-neighbour coupling configuration. There are four such sublattices for our alternating coupling Ising model (but only two for the related chess-board model and one for the Onsager problem). The function $W_L^{aa',\alpha\alpha'}(\boldsymbol{x}, \boldsymbol{x}')$ satisfies the integral equation

$$W_L^{aa',\alpha\alpha'}(\boldsymbol{x}, \boldsymbol{x}') = \sum_{\boldsymbol{y},b,\beta} B^{ab,\alpha\beta}(\boldsymbol{x}, \boldsymbol{y}) W_{L-1}^{ba',\beta\alpha'}(\boldsymbol{y}, \boldsymbol{x}') \tag{2.7}$$

implying that a path of L bonds can be constructed from a path of $(L-1)$ bonds via all intermediate configurations. The contribution from closed paths is obtained by taking the trace of W_L, except that in this way a closed loop contributing to $f_N(L)$ appears $2L$ times:

$$f_N(L) = \frac{1}{2L} \sum_{\boldsymbol{x},a,\alpha} W_L^{aa,\alpha\alpha}(\boldsymbol{x}, \boldsymbol{x}) = \frac{1}{2L} b_N(L) \tag{2.8}$$

so that for the partition function we obtain

$$\mathcal{Z}_1 = \sum_{s=0}^{\infty} \frac{(-1)^s}{2^s s!} \left(\sum_{L=0}^{\infty} \frac{b_N(L)}{L} \right)^s = \exp\left(-\frac{1}{2} \sum_{L=0}^{\infty} \frac{b_N(L)}{L} \right). \tag{2.9}$$

In order to calculate the trace $b_N(L)$ of $W_L^{aa',\alpha\alpha'}(\boldsymbol{x},\boldsymbol{x}')$ we notice that this function remains invariant for translations of $\boldsymbol{x}$ and $\boldsymbol{x}'$ by a lattice vector $\boldsymbol{z}$ that leaves the sites in the same sublattices. This means that the function is invariant for translations within a single sublattice, and consequently equation (2.7) can be rewritten in terms of the Fourier coefficients of W and B:

$$W_L^{aa',\alpha\alpha'}(\boldsymbol{p}) = \sum_{b,\beta} B^{ab,\alpha\beta}(\boldsymbol{p}) W_{L-1}^{ba',\beta\alpha'}(\boldsymbol{p}) \tag{2.10}$$

where

$$B^{ab,\alpha\beta}(\boldsymbol{p}) = \sum_{\boldsymbol{y}} B^{ab,\alpha\beta}(\boldsymbol{x},\boldsymbol{y}) \mathrm{e}^{\mathrm{i}\boldsymbol{p}(\boldsymbol{x}-\boldsymbol{y})}. \tag{2.11}$$

Iterating equation (2.11) L times, we arrive at

$$W_L^{aa',\alpha\alpha'}(\boldsymbol{p}) = \sum_{b_1,\cdots,b_{L-1}} \sum_{\beta_1,\cdots,\beta_{L-1}} B^{ab_1,\alpha\beta_1}(\boldsymbol{p}) \cdots B^{b_{L-1}a',\beta_{L-1}\alpha'}(\boldsymbol{p}) = \left(B(\boldsymbol{p})^L\right)^{aa',\alpha\alpha'}. \tag{2.12}$$

Since the translational invariance applies to a quarter of the total number of sites, we have, always in the limit $N \to \infty$:

$$b_N(L) = \sum_{\boldsymbol{x},a,\alpha} W_L^{aa,\alpha\alpha}(\boldsymbol{x},\boldsymbol{x}) = \sum_{\boldsymbol{p},a,\alpha} W_L^{aa,\alpha\alpha}(\boldsymbol{p}) = \sum_{\boldsymbol{p}} \mathrm{Tr}\left(B(\boldsymbol{p})^L\right) \tag{2.13}$$

and inserting equation (2.13) into equation (2.9) we obtain

$$\begin{aligned} \frac{F_1}{T} &= -\ln \mathcal{Z}_1 = \frac{1}{2} \sum_{\boldsymbol{p}} \mathrm{Tr}\left(\sum_{L=0}^{\infty} \frac{B(\boldsymbol{p})^L}{L} \right) \\ &= -\frac{N}{2(2\pi)^2} \int_{-\pi/2}^{\pi/2} \mathrm{d}^2 p \, \ln[\det(1 - B(\boldsymbol{p}))]. \end{aligned} \tag{2.14}$$

The problem is again reduced to the determination of the matrix $B(\boldsymbol{p})$. Here, defining the superindex $\mu = (a,\alpha)$, we see that, in principle, we have to evaluate a 16×16 matrix. However the matrix can be reduced in size, since any site can be reached in one step only from its four nearest neighbours which belong to just two of the four possible sublattices. A similar reduction applies to the orientations, and thus the matrix $\mathbf{B}$ must have the form

$$\mathbf{B} = \begin{pmatrix} 0 & B_1 \\ B_2 & 0 \end{pmatrix} \tag{2.15}$$

where B_1 and B_2 are 8×8 matrices such that $\det(1 - \mathbf{B}) = \det(1 - B_1 B_2)$. The calculation of B_1 and B_2 proceeds as in Vdovichenko's paper, and we obtain:

$$B_1 B_2 = \begin{pmatrix} A_{11} & A_{12} \\ A_{21} & A_{11} \end{pmatrix} \tag{2.16}$$

with

$$A_{11} = \begin{pmatrix} t_1 t_2 e^{-2ip} & 0 & \alpha^{-1} t_3 t_4 e^{-2iq} & \alpha t_3 t_4 e^{2iq} \\ 0 & t_1 t_2 e^{2ip} & \alpha t_3 t_4 e^{-2iq} & \alpha^{-1} t_3 t_4 e^{2iq} \\ \alpha t_1 t_2 e^{-2ip} & \alpha^{-1} t_1 t_2 e^{2ip} & t_3 t_4 e^{-2iq} & 0 \\ \alpha^{-1} t_1 t_2 e^{-2ip} & \alpha t_1 t_2 e^{2ip} & 0 & t_3 t_4 e^{2iq} \end{pmatrix} \tag{2.17}$$

$$A_{12} = \begin{pmatrix} t_2 t_a(q) e^{-ip} & \alpha^2 t_1 t_b(q) e^{ip} & \alpha^{-1} t_2 t_3 e^{-i(p+q)} & \alpha t_2 t_4 e^{-i(p-q)} \\ -\alpha^2 t_2 t_b(q) e^{-ip} & t_1 t_a(q) e^{ip} & \alpha t_1 t_3 e^{i(p-q)} & \alpha^{-1} t_1 t_4 e^{i(p+q)} \\ \alpha t_2 t_3 e^{-i(p+q)} & \alpha^{-1} t_1 t_3 e^{i(p-q)} & t_3 t_c(p) e^{-iq} & \alpha^2 t_4 t_d(p) \\ \alpha^{-1} t_2 t_4 e^{-i(p-q)} & \alpha t_1 t_4 e^{i(p+q)} & -\alpha^2 t_3 t_d(p) e^{-iq} & t_4 t_c(p) e^{iq} \end{pmatrix} \tag{2.18}$$

where

$$t_a(q) = t_3 e^{-iq} + t_4 e^{iq} \qquad t_b(q) = -t_3 e^{-iq} + t_4 e^{iq}$$

$$t_c(p) = t_2 e^{-ip} + t_1 e^{ip} \qquad t_d(p) = t_2 e^{-ip} - t_1 e^{ip}$$

and where α denotes $e^{i\pi/4}$ and $(p, q) = \boldsymbol{p}$. A_{21} is obtained from A_{12} by interchanging t_1 with t_2 and t_3 with t_4.

The order–disorder phase transition of interest corresponds to the vanishing of one of the eigenvalues of $1 - B(\boldsymbol{p})$ for $p = 0$, $\pi/2$ and $q = 0$, which places the transition in the expected two-dimensional Ising universality class. Let us point out that the particular wavevector p component leading to a vanishing determinant is related to the modulation of the ground state; i.e. for $\kappa > 0$ we have the antiphase ($\langle - + + - \rangle$, $\langle + - - + \rangle$) with a periodicity of four lattice spacings (two sublattice spacings), and hence $p = \pi/2$; while for $\kappa < 0$ we have the ferromagnetic phase ($\langle + + + + \rangle$) with a periodicity of one lattice spacing, and hence $p = 0$ (or $p = \pi$). This is for the soft direction, while for the hard direction the periodicity is always of one lattice spacing, and hence $q = 0$. Were it not for the unenforced six-vertex constraint, the transition could be identified with reconstruction; notice, however, that this would also be present for $\kappa < 0$ in this model. The Ising transition lines are reported in figure 2, which were obtained by numerical solution of the equation $\det(1 - B(0, 0)) = 0$ for T_c as function of $\kappa < 0$, and $\det(1 - B(\pi/2, 0)) = 0$ for $\kappa > 0$ (with $\alpha = 0.75$ in model (1.1)).

The availability of an exact solution for T_c allows us to test our transfer matrix methods to be used for later numerical studies. Here we choose to use the iteration scheme of Cheung and McMillan (1983) for the determination of the matrix eigenvalues. In this scheme the transfer-matrix for a strip of width n,

$$T_{(n)}(\Sigma_j, \Sigma'_{j+1}) = \prod_{i=1}^{n} \exp\left(K_{ij,ij+1} s_{ij} s'_{ij+1} + K_{ij,i+1j} s_{ij} s_{i+1j}\right) \tag{2.19}$$

is replaced by an (analytic) iteration relation for the amplitudes $a(m_1, \ldots, m_n)$ of the 2^n-dimensional vectors $v(\Sigma_j)$ upon which the transfer-matrix acts. These amplitudes arise from the representation

$$v_j(\Sigma_j) = \sum_{m_1, \ldots, m_n = 0,1} a_j(m_1, \ldots, m_n) s_{1j}^{m_1} \cdots s_{nj}^{m_n} \tag{2.20}$$

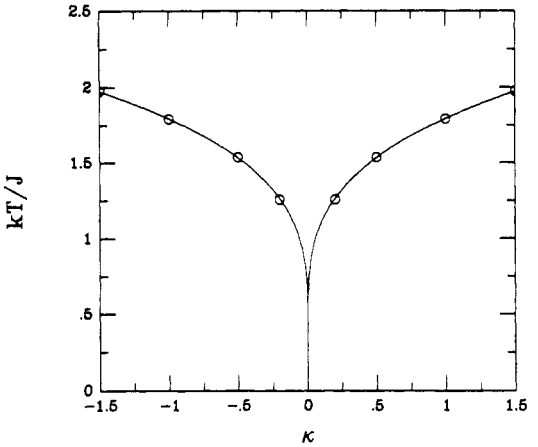

Figure 2. Phase diagram for the model Hamiltonian (1.1) when the height conservation constraint is relaxed and all Ising configurations are allowed ($\lambda = 0$). Full lines denote the exact two-dimensional Ising transition lines, empty circles the results from the finite-size scaling analysis.

of a vector in terms of spin operators, which has the advantage of providing an exact separation of the eigenvector space into even and odd subspaces with respect to the global spin-reversal transformation $\{s_{ij}\} \rightarrow \{-s_{ij}\}$, separation which is preserved by our spin-reversal invariant Hamiltonian (2.1). The two dominant eigenvalues λ_1 and λ_2 (with $|\lambda_1| > |\lambda_2|$) then arise from iteration of amplitudes associated with the two orthogonal subspaces via the application of some iterated power method (Wilkinson 1965). The amplitude iteration relation arises from the application of the transfer-matrix to an arbitrary vector

$$\sum_{k_1,\ldots,k_n=0,1} a_{j+1}(k_1,\ldots,k_n) s'^{k_1}_{1j+1}\cdots s'^{k_n}_{nj+1}$$

$$= \sum_{m_1,\ldots,m_n=0,1} a_j(m_1,\ldots,m_n) \prod_{i=1}^{n} (u_{ij,i+1j} u_{ij,ij+1})$$

$$\times \sum_{\{s_{ij}=\pm 1\}} \prod_{i=1}^{n} (1 + t_{ij,i+1j} s_{ij} s_{i+1,j})(1 + t_{ij,ij+1} s_{ij} s'_{ij+1}) s_{ij}^{m_i} \tag{2.21}$$

where $u_{ij,kl} = \cosh(K_{ij,kl})$, resulting in the iteration relation

$$a_{j+1}(k_1,\ldots,k_n) = \sum_{m_1,\ldots,m_n=0,1} c_j(k_1,\ldots,k_n; m_1,\ldots,m_n) a_j(m_1,\ldots,m_n). \tag{2.22}$$

For the alternating coupling Ising Hamiltonian (2.1), the recursion relation has the form:

$$c_j(\boldsymbol{k},\boldsymbol{m}) = (u_1 u_2)^{n/2} u_j^n t_j^{\sum_{i=1}^{n} k_i} D_j(K_1, K_2, \boldsymbol{k}, \boldsymbol{m}) \qquad j = 3, 4 \tag{2.23}$$

where the index j refers to the column in the iteration along a diagonal strip and indicates that two distinct matrices are required in the iteration. The function

$D_j(K_1, K_2, \boldsymbol{k}, \boldsymbol{m})$ in equation (2.23) is given by

$$D_j(K_1, K_2, \boldsymbol{k}, \boldsymbol{m}) = \sum_{\{s_i=\pm 1\}} A_j(\{s_i\}, K_1, K_2) s_1^{k_1+m_n} s_2^{k_2+m_1} \dots s_n^{k_n+m_{n-1}} \tag{2.24}$$

where

$$A_3(\{s_i\}, K_1, K_2) = (1 + t_1 s_1 s_2)(1 + t_2 s_2 s_3)(1 + t_1 s_3 s_4) \dots (1 + t_2 s_n s_1) \tag{2.25}$$

and $A_4(\{s_i\}, K_1, K_2) = A_3(\{s_i\}, K_2, K_1)$, indicating the alternancy of the coupling structure, thus of the transfer-matrix, along the direction of transfer. To compute D_j, observe that equation (2.24) implies the trace over the whole set of spin variables of products of the type $A_j(\{s_i\}) s_1^{p_1} \cdots s_n^{p_n}$, with $p_i = 0, 1$. The parity of a spin configuration is given by the parity of the quantity $k = \sum_{i=1}^n k_i$. Since the global spin-reversal invariance implies that the transfer-matrix elements between different parity configurations must vanish, we see that $p = \sum_{i=1}^n p_i = k + m = \sum_{i=1}^n (k_i + m_i)$ must be an even number, and hence the number of p_is taking a value 1 must also be even. Let us denote by $(r_1, \dots, r_p)$ the sequence of places in the ordered sequence $(p_1, \dots, p_n)$ corresponding to a 1. Now, a rather cumbersome calculation provides the desired result in terms of the r-sequence:

$$D_3(t_1, t_2, \boldsymbol{k}, \boldsymbol{m}) = 2^n \left(t_1^{\alpha} t_2^{\gamma} + t_1^{((n/2)-\alpha)} t_2^{((n/2)-\gamma)} \right). \tag{2.26}$$

In equation (2.24), D_3 is the trace of the function $A_3(\Sigma, K_1, K_2)$ multiplied by a product of spins. The sum of the exponents of these spins is $p = k + m$; if p is odd, global spin-reversal invariance implies $D_3 = 0$, otherwise the number p, together with the binary vectors $\boldsymbol{k}$ and $\boldsymbol{m}$, defines the r-sequence and consequently the exponents α and γ in the following way. The power α is the number of K_1 interactions within $(1, r_1) \cup (r_2, r_3) \cup \cdots \cup (r_p, n)$ in the column of spins attached to equation (2.25), and γ is the number of K_2 interactions in the same set, plus one (counting the K_2 interaction between s_1 and s_n). The other powers, $((n/2) - \alpha)$ and $((n/2) - \gamma)$, correspond to the complement of the set above. As before, $D_4(K_1, K_2, \boldsymbol{k}, \boldsymbol{m}) = D_3(K_2, K_1, \boldsymbol{k}, \boldsymbol{m})$. Once the iteration relations $c_j(\boldsymbol{k}, \boldsymbol{m})$ are specified, repeated iterations $\cdots c_3 c_4 c_3 c_4 \cdots$ on an amplitude vector belonging to either even or odd eigenspace yields the appropriate eigenvalue λ_k. The advantage of the transfer-matrix method of Cheung and McMillan is that the iterations can be carried out analytically and no re-orthogonalization is ever needed to keep the two subspaces separate. As usual the eigenvalues yield both the free energy per site $f(T)$ and the correlation length $\xi(T)$ via the equations

$$f_n(T) = -\frac{T}{2n} \ln \lambda_1 \qquad \xi_n(T) = \left[\ln \left(\frac{\lambda_1}{\lambda_2} \right) \right]^{-1} \tag{2.27}$$

where λ_1 and λ_2 are the two dominant eigenvalues of $T_3 T_4$.

By making use of the phenomenological renormalization prescription for the correlation length,

$$\frac{\xi_n(T^*)}{n} = \frac{\xi_m(T^*)}{m} \tag{2.28}$$

an estimate for the position of the critical point of the transition can be obtained. We have carried out iterations for model (1.1) in the $\lambda = 0$ limit, with $\alpha = 0.75$ and

for sizes $n = 4, 8, 12$ for $\kappa > 0$ (n is a multiple of 4 in order to avoid parity problems associated with the 1×2 ground state), and $n = 4, 6, 8, 10$ for $\kappa < 0$. The extrapolated results are also reported in figure 2 (assuming the standard two-dimensional Ising corrections to scaling in order to perform the extrapolation) for some values of κ. Comparison with the exact boundary lines demonstrate the accuracy of our numerical transfer-matrix approach.

3. Finite-size scaling and phase diagram for the constrained Hamiltonian ($\lambda = \infty$)

We now come to the analysis of the physical limit for model Hamiltonian (1.1), where the six-vertex constraint is enforced on all the square cells of the spin lattice in order to recover height conservation for closed arbitrary paths, i.e. we now deal with $\lambda = \infty$ in (1.3).

We have studied the phase behaviour of the model through the method of finite-size scaling (Nightingale 1981, Barber 1983) applied to the exact numerical evaluation of thermodynamic surface properties for infinite one-dimensional lattice strips. Height conservation is imposed in the determination of the matrix elements and eigenvalues. The transfer-matrix elements for Hamiltonian (1.1) in this limit, are defined by equation (2.19) for all configurations Σ and Σ' compatible with each other through the six-vertex constraint, and are zero otherwise. In our case, convergence for increasing n is fastest for a transfer in the diagonal direction, and the full transfer-matrix breaks down in the product of two matrices alternating in the direction of transfer, due to the alternancy of the interactions. The height difference at column j between the two strip edges is given by

$$\Delta h_j = \sum_{i=1}^{n} (-1)^{i+1} s_{ij} \tag{3.1}$$

so that the height conservation rule, equation (1.2), automatically implies that $\Delta h_j = \Delta h_{j+1}$ for periodic boundary conditions in the direction orthogonal to the transfer. The full matrix is consequently of block-diagonal form, each block corresponding to a particular height difference (Lieb and Wu 1972, Baxter 1982). Thus, we evaluate the free energy per site from the largest eigenvalue of the central block ($\Delta h = 0$)

$$f(\kappa, T) = -\frac{T}{2n} \ln(\lambda_1^{(0)}) \tag{3.2}$$

whilst the free energy for step formation is given by

$$f_s^*(T) = -\frac{T}{2} \ln\left(\frac{\lambda_1^{(2)}}{\lambda_1^{(0)}}\right) \tag{3.3}$$

with $\lambda_1^{(2)}$ the dominant eigenvalue of the subcentral block ($\Delta h = 2$). The results obtained for the heat capacity per site are shown in figure 3 for strips of sizes $n = 4, 6, 8, 10$ as a function of temperature for $\kappa < 0$. Similar results are shown in figure 4 for $\kappa > 0$, although in this case convergence suffers from parity effects owing to the symmetry of the 1×2 ground state and consequently only results for

strip sizes $n = 4, 8$ are shown. There is a peak for all values of κ, the peak's temperature falling for decreasing $|\kappa|$. For $\kappa > 0$, the peak should be identified with the deconstruction transition, while for $\kappa < 0$ with an order–disorder transition as discussed in the introduction. For sufficiently small values of $|\kappa|$, the finite-size scaling of the peak very closely resembles an Ising transition. On the other hand, for large $|\kappa|$ (of the order of α), the heat capacity peak appears to be saturating with increasing n, perhaps an indication for the drifting of the related critical exponent towards the Kosterlitz–Thouless value $-\infty$. A possible explanation stems from the fact that, while the energy of stepped defects is of order α, that of flat ones is of order $|\kappa|$. Hence, for $|\kappa| \ll \alpha$ reconstruction involves mostly in-plane degrees of freedom, whilst for larger $|\kappa|$s competition with off-plane degrees of freedom will modify the nature of the reconstruction transition for $\kappa > 0$. In figure 5 (lower curve) the position of the peak in the heat capacity is drawn as function of size n and anisotropy κ. For very small values of $|\kappa|$, severe finite-size effects come into play, as the system becomes strongly quasi-one-dimensional. However there is indication that the curves approach the origin with infinite slope. For $\kappa \simeq -0.4$ the position of the peak appears to be independent of the size n, thus its value is determined exactly to numerical precision. For $\kappa = -2\alpha$, the model becomes exactly isomorphic to an anisotropic BCSOS model. For a BCSOS model we know there is no second-order transition but instead an infinite-order transition preceded by a peak in the heat capacity, whose position can be determined exactly†. We point out that precisely for $\kappa = -2\alpha$ our model recovers symmetry between h and l inequivalent layer sites. Through the above exact points a fitting curve has been drawn in figure 5 in order to give a possible indication of the convergence of our finite-size evaluation.

The position of the roughening transition in our model for $\kappa = -2\alpha$ can also be determined numerically, by extrapolating the temperature dependence of the step free energy f_s to $n = \infty$ and determining the temperature T_R where f_s vanishes. Good agreement is obtained with the exact result for the BCSOS model, though this method is not very precise for determining the roughening temperature (Luck 1981). For $\kappa > -2\alpha$, a faster and more accurate convergence is obtained from the calculation of the following approximant to f_s

$$g_s(\kappa, T) = -\frac{T}{2} \ln \left(\frac{\lambda_2^{(0)}}{\lambda_1^{(2)}} \right) \tag{3.4}$$

where $\lambda_2^{(0)}$ represents the subdominant eigenvalue of the central block. g_s is an approximant to f_s in that $\lambda_1^{(0)}$ becomes degenerate with $\lambda_2^{(0)}$ in the thermodynamic limit. However, g_s becomes negative for $T > T_R$ in finite-size systems, thus allowing for a more precise evaluation of T_R. The resulting curves are given in figure 5 (upper curves), which complete our phase diagram.

It is interesting to notice the improvement of the convergence of the sequence $\{T_R(n)\}$ towards T_R as a function of increasing n, as soon as the parameters of the model approach those of the BCSOS model. Indeed, for $\kappa = -2\alpha$, already the smallest size $n = 4$ gives the correct value to numerical accuracy. Since this result remains

† In this case, the surface energy anisotropy parameter would be $\nu = \alpha^{-1} = (e_1 - e_5)/(e_3 - e_5)$, with e_i the vertex energies. Trayanov *et al* (1989, 1990) have previously presented a mapping of non-reconstructing FCC [110] surfaces onto an anisotropic BCSOS model. The present model can be regarded as an extension of theirs to include reconstruction tendencies.

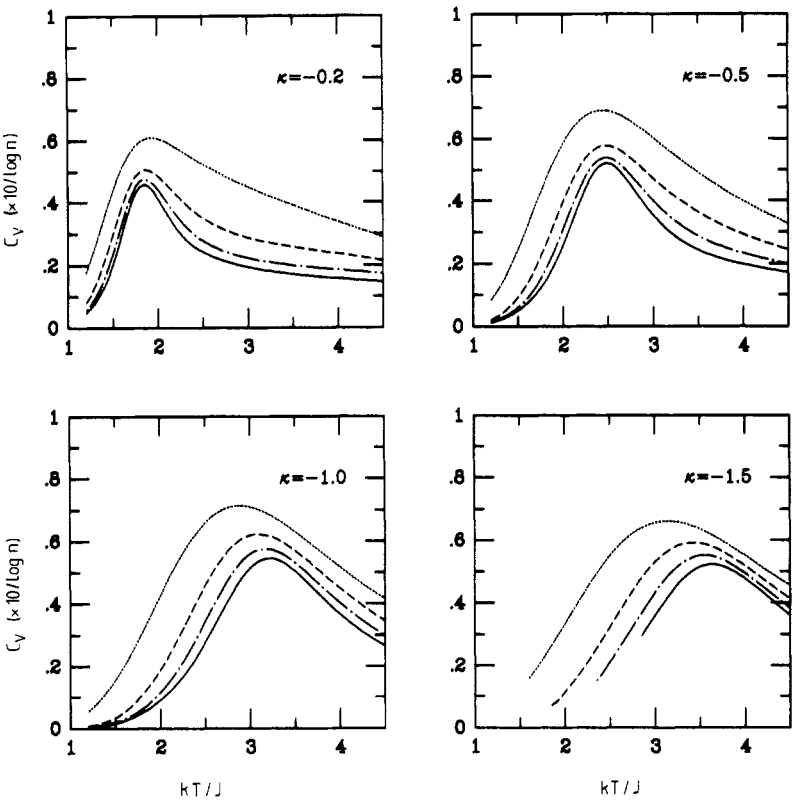

Figure 3. Finite-size and temperature dependence of the scaled heat capacity per site for non-reconstructing surfaces (1 x 1). Dotted line, $n = 4$; broken line, $n = 6$; chain line, $n = 8$; full line, $n = 10$.

practically the same when size is increased, one can say that stepping in this model is a completely local phenomenon, in the sense that the interaction energy between neighbouring steps vanishes. The departure from the BCSOS model implies, therefore, that steps become interacting.

As for the nature of the roughening transition, we point out that our model resembles that studied by Knops (1979), in which two anisotropic compenetrating SOS lattices are constrained precisely by the same $h_{ij} - l_{i'j'} = \pm 1$ condition on neighbouring columns. Knops proposes that, except for the non-alternating case, the transition should be Ising-like and occur under limited total height difference, whilst true roughening takes place at $T = \infty$. Here we see, from heat capacity studies, that by varying κ the thermal exponent could change almost continuously, probably indicating the existence of weak universality conditions (Suzuki 1974). Also, the vanishing of the step free energy points to a true roughening transition at finite temperature. Naturally, much larger strip sizes should be considered in order to confirm our suggestion. We should stress here the difference between the roughening curve pertaining to the present model and that determined by Jug and Tosatti (1990) for the original discrete Gaussian version of the model. In the case of the unrestricted model all height jumps are, in principle, allowed between neighbouring atomic columns, yielding a Kosterlitz–

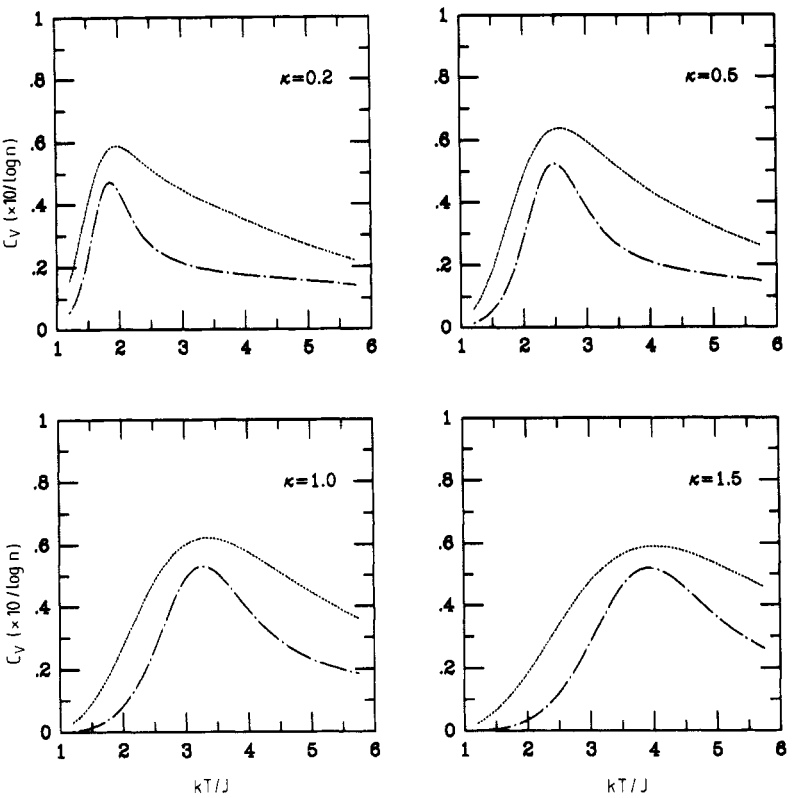

Figure 4. As in figure 3, but for reconstructing surfaces (1 x 2).

Thouless transition temperature $T_R(\kappa)$ vanishing for $\kappa > 2\alpha$. For the present model, the restriction on the value of height jumps between sites of the two coupled six-vertex sublattices leads to a quite different behaviour, as was first advocated in the work of Knops (1979).

4. The lambda model: a continuous path from unconstrained to constrained Hamiltonians

So far we have studied the phase diagram of the Hamiltonian (1.1) both in the unconstrained limit ($\lambda = 0$), i.e. where condition (1.2) is completely relaxed; and in the constrained limit ($\lambda = \infty$), i.e. where condition (1.2) is rigorously verified. The first case was shown to present just a second-order phase transition of the Ising universality class. The other, the BCSOS limit, presents a pseudo order–disorder phase transition at low temperatures, and a clear roughening transition at a higher temperature. Our aim in this section is to analyse the intermediate behaviour as a function of λ; i.e. when condition (1.2) is partially relaxed through the additional term $\mathcal{H}_\square$ given by equation (1.3). For the sake of simplicity, as well as for its own intrinsic interest, we

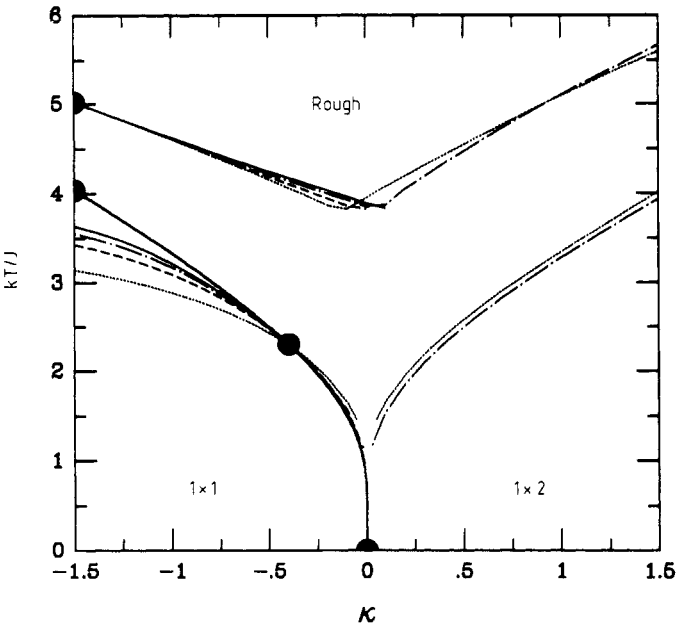

Figure 5. Suggested phase diagram for the model Hamiltonian (1.1) with the six-vertex constraint enforced ($\lambda = \infty$). The upper curves are for the smooth–rough transition; the lower curves represent the position of the roughening peak for $\kappa < 0$, and of the Ising-like order–disorder transition for $\kappa > 0$. Curves as in figure 4.

choose to replace (1.1) with the simpler isotropic non-alternate Ising form

$$\mathcal{H}(\lambda) = -J \sum_{i,j} \{s_{i,j}s_{i+1,j} + s_{i,j}s_{i+1,j}\} + \lambda \sum_{\square} (s_{i,j} - s_{i+1,j} - s_{i,j+1} + s_{i+1,j+1})^2. \quad (4.1)$$

We therefore study by the transfer-matrix technique the λ-model (4.1) connecting the pure two-dimensional Ising model ($\lambda = 0$) with the F-model ($\lambda = \infty$) (Rys 1963).

It is useful for what concerns the computational scheme to expand the squares in the second term of (4.1), in order to obtain a Hamiltonian composed just of two-body interactions. Besides a trivial constant part, the Hamiltonian reads

$$\mathcal{H}(\lambda) = -(J + 2\lambda) \sum_{i,j} \{s_{i,j}s_{i+1,j} + s_{i,j}s_{i,j+1}\} + 2\lambda \sum_{\{i,j\}\ \text{even}} \{s_{i,j}s_{i+1,j+1} + s_{i+1,j}s_{i,j+1}\}. \quad (4.2)$$

A schematic representation of model (4.2) is shown in figure 6.

We have studied two separate aspects of this model. The first is the behaviour of the correlation length as a function of temperature for various sizes. This allows for the possibility of following the continuous evolution from the Ising transition at $T_c(\lambda = 0)$ towards the Kosterlitz–Thouless one at $T_R(\lambda = \infty)$. Moreover, we have been able to calculate the thermal critical exponent ν, characterizing the universality class of the transition. The second is a study of the approximant to the effective step free energy close to the six-vertex limit (i.e. for small values of λ^{-1}). The temperature where this quantity vanishes is used to identify a renormalized roughening temperature $T_R(\lambda)$,

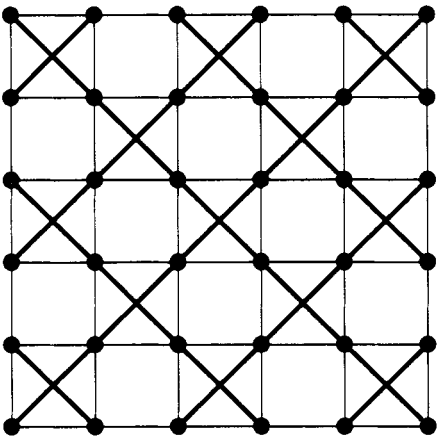

Figure 6. Schematic representation of the couplings involved in the λ-model. Circles are sites of the spin lattice; light lines represent first neighbour couplings of strength $-(J + 2\lambda)$, and bold lines, second neighbour couplings of strength 2λ.

at least as far as the character of the eigenvectors associated with the eigenvalues $\lambda_1^{(2)}$ and $\lambda_2^{(0)}$ can still be thought of as representing an average global height jump of 2 and 0 lattice spacings respectively.

4.1. Order–disorder transition

We have studied the finite-size scaling behaviour of the correlation length, obtained via the ratio between dominant and subdominant eigenvalues of the transfer-matrix for finite systems of sizes 4, 6, 8 and 10 sites; using the second equation in (2.27). The resulting phase diagram is shown in figure 7, where it becomes clear that the well known Ising transition at $T_c = 2/\ln(1+\sqrt{2})$ (Onsager's result) for $\lambda = 0$, moves upwards with increasing λ in order to achieve the value $T_R = 4/\ln 2$ (Lieb and Wu's result) for $\lambda \to \infty$. Actually, in this last limit the value obtained for T_c is slightly smaller than T_R, due to the fact that the definition of correlation length used is not the correct one. When $\lambda \to \infty$ we have to use for the correlation length the inverse of the step free energy, given by equation (3.3). From the derivative of the correlation length with respect to temperature we have calculated the critical exponent ν, through the formula

$$1 + \frac{1}{\nu_{n,n+2}} = \frac{\ln[\xi'_{n+2}(T^*_{n,n+2})/\xi'_n(T^*_{n,n+2})]}{\ln[(n+2)/n]} \tag{4.3}$$

where ξ' is the previously mentioned derivative, and $T^*_{n,n+2}$ is the estimate for the transition temperature corresponding to the crossing of the scaled correlation lengths for sizes n and $n+2$. In the Ising limit, we know that $\nu(\lambda = 0) = 1$ (Onsager 1944); while in the six-vertex limit ν is no more well defined since the correlation length diverges exponentially, instead of with a power-law. This kind of behaviour, if one insisted on computing ν with formula (4.3), would be consistent with a value $\nu(\lambda \to \infty) \to \infty$, which is indeed verified in the sense of a trend for increasing size, as can be seen in figure 8 where we present our results for the critical exponent ν in the λ-model, as a function of λ for different sizes. The main result of this analysis is that

this model has a non-universal critical behaviour, reflected by a thermal exponent ν continuously varying with λ. In particular, there is a point at $\lambda \sim 2.6$, where a lack of corrections to finite-size scaling allows us to identify a critical exponent $\nu \simeq 0.85$, different from Onsager's $\nu = 1$. Let us note, by the way, that smaller values of ν are characteristic of systems with a smaller number of degrees of freedom.

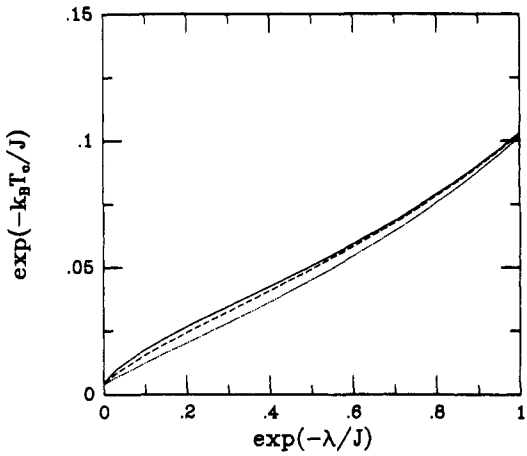

Figure 7. Phase diagram for the λ-model as resulting from the finite-size scaling of the correlation length with sizes n and $n + 2$. The phase boundary is characterized by a continuously varying thermal critical exponent ν. The upper phase (low-temperature) is ordered, and the lower one (high-temperature) is disordered, in terms of spin variables. The dotted line is for $n = 4$, the broken line for $n = 6$ and the full line for $n = 8$.

It is also interesting to analyse the behaviour of the peak in the heat capacity, another estimator for the transition temperature. We have performed this calculation by means of the first equation in (2.27) and present a plot of the peak's temperature in figure 9. It should be noticed the close relation of this phase diagram with that of figure 7, showing the critical temperature as obtained from the correlation length. Moreover, for $\lambda \sim 0.3$, corrections to finite-size scaling seem to disappear, thus allowing for the accurate determination of one point in this phase diagram. By increasing λ the peak broadens while decreasing in height (in order to preserve the integral of the heat capacity per site), thus indicating the crossover from a situation with a true thermodynamic-limit divergence in C_V (for small λ), to a system where the heat capacity is non-divergent (for large λ). Another feature of the heat capacity is that for large enough values of λ, the peak appears to be made up by two peaks at different temperatures. The lower-temperature peak approaches (for $\lambda \to \infty$) the behaviour found in six-vertex models (figure 3, $\kappa = -1.5$), though it represents the isotropic BCSOS model. The higher-temperature peak seems to shift to infinity for $\lambda \to \infty$, but its position strongly decreases with the size, in such a way that, when extrapolated for $n \to \infty$, it seems to merge with the other peak. Since this occurs for values of $\lambda > 8$ it is not visible in the plot of the phase boundaries. However, this portion of the phase diagram is magnified in the inset of figure 9. Nevertheless, from these studies of the heat capacity it is very difficult to be conclusive about the nature of the transition in the whole range of λ. This is due to the finiteness of the systems under consideration, and to the fact that the finite-size scaling behaviour of a marginal operator—like the

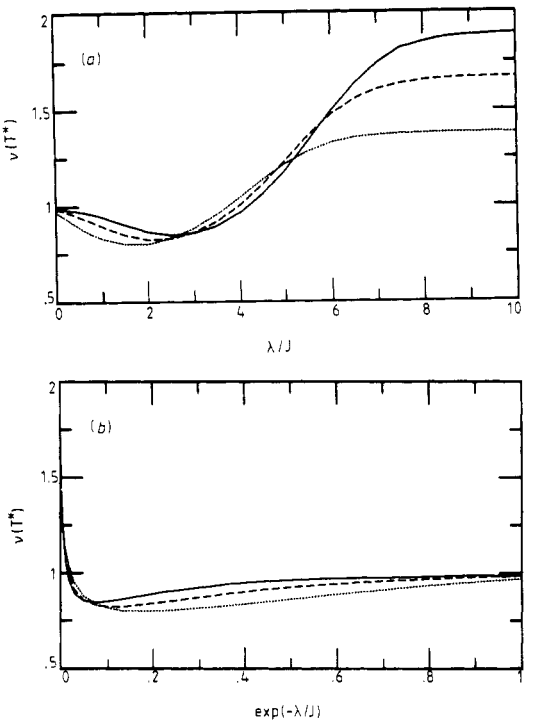

Figure 8. Thermal critical exponent ν as a function of (a) λ and (b) $\exp(-\lambda/J)$. For $\lambda \to \infty$ the finite-size ν strongly increases with size, probably indicating an approach to $\nu \to \infty$ consistent with a Kosterlitz–Thouless phase transition. The meaning of the three lines is the same as in figure 8.

energy operator—is controlled by corrections to scaling (Nightingale 1981).

4.2. Roughening transition

Conversely to what was done in section 4.1, we can start from $\lambda \to \infty$, which we know to correspond to the case of the F-model, and then progressively reduce the value of λ. Since for $\lambda \to \infty$ T_R is determined through equation (3.4), we could, in principle, assume that for λ sufficiently large (3.4) is still a good operational definition for a renormalized roughening temperature ($T_R(\lambda)$), although strictly speaking the height is no longer a well-defined variable at each lattice site. Nevertheless, for small λ^{-1}, the six-vertex constraint violations must occur in a limited fashion; i.e. a single violation along the short strip direction is represented by the inclusion of an off-diagonal transfer-matrix block element of the order $\Lambda = \exp(-4\lambda/T)$. These will be the matrix elements connecting blocks (of a block-diagonalized matrix) having different global height jumps, with a ± 2 difference in Δh between the blocks (i.e. central ($\Delta h = 0$) and subcentral ($\Delta h = \pm 2$) blocks; $\Delta h = \pm 2$ and $\Delta h = \pm 4$ blocks, etc). At the same time, double but opposite sign violations can occur inside a particular block, thus giving rise to elements of order Λ^2. The λ-model includes all Ising configurations, but weighted with a factor $\Lambda^{qk/4}$, k being the number of six-vertex constraint violations along the short direction of the strip, and $q = s_{i,j} - s_{i+1,j} - s_{i,j+1} + s_{i+1,j+1}$ the topological charge of the violating 4-spin plaquette (figure 1(a)) configuration (note that the six configurations shown in figure 1(b) all have charge $q = 0$).

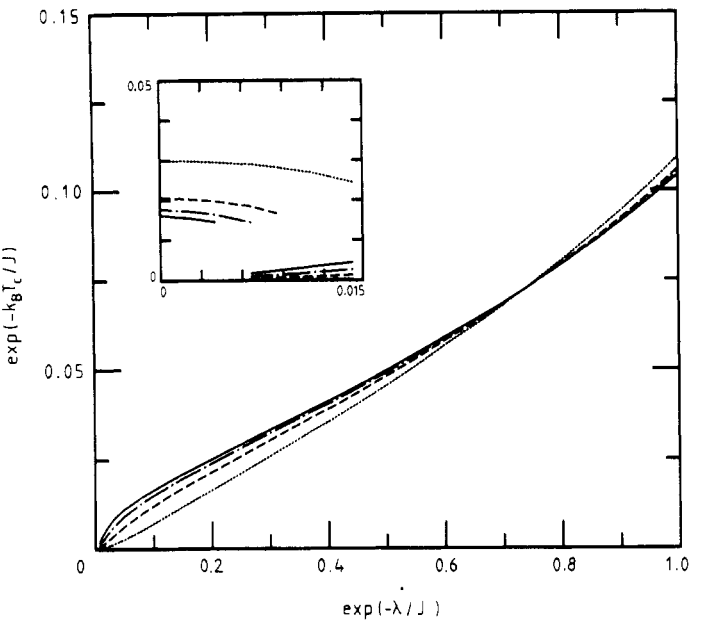

Figure 9. Phase diagram for the λ-model as resulting from a study of the peak in the heat capacity. The dotted line is for $n = 4$, the broken line for $n = 6$, the chain line for $n = 8$, and the full line for $n = 10$. The inset is a magnification of the region of large values of λ.

Based on these considerations we can think of the λ-model (in the limit of small λ^{-1}) as representative of a surface in the presence of a small density of bulk dislocations, although these are not frozen in space (as is the usual case for screw dislocations propagating from the bulk), but are included in the statistical framework. In this sense, the model represents an alternative to Baxter's eight-vertex model (van Beijeren 1977, Knops 1979) where just topological charges (Burgers vectors) $q = 0, 4$ are taken into account. The main point concerning the interpretation of the temperature arising from equation (3.4), would be that the eigenvalues must preserve, on average, a well-defined global height jump between the two ends of the strip, not very far from 0 ($\lambda_2^{(0)}$) and 2 ($\lambda_1^{(2)}$). A measure of this departure is given by

$$\langle \Delta_{m,k} \rangle = \sum_{i=1}^{N} \left(v_i^{(m,k)} \right)^2 \delta_{\Delta h_i, m} \tag{4.4}$$

where the $v_i^{(m,k)}$ are the components of the eigenvector corresponding to the eigenvalue $\lambda_k^{(m)}$, in the orthonormal basis formed by column configurations (dimension $N = 2^n$, with n the size of the strip). The quantity Δh_i is the global height jump associated with configuration i. Hence, we are counting the proportion of m-like states in those eigenvectors.

We have carried out the calculation of $T_R(\lambda)$ through equation (3.4) for strips of sizes $n = 4, 6, 8$ and 10, and we present the resulting renormalized roughening temperature as a function of λ in figure 10. Two main aspects are to be stressed. The

first one is that in the λ-model, where the alternancy of the interactions is removed, the temperature $T_R(\lambda, n)$ turns out to be size-independent as in the BCSOS model; i.e. the pseudo-steps are non-interacting. The second concerns the behaviour of $T_R(\lambda)$ as a function of λ, and it can be seen that the roughening temperature shows a practically constant region down to $\lambda \simeq 1.5$. For values of $\lambda < 1.5$, $T_R(\lambda)$ is seen to grow very rapidly. Moreover, although for $\lambda = 0$ the concept of height is ill defined, if one insists on looking at the behaviour of the zero of equation (3.4), the latter will turn out to occur at infinite temperature †. Therefore, the Ising transition of the unconstrained Hamiltonian (2.1) cannot be identified with a roughening transition, but it represents rather well the in-plane disordering of a surface, despite the fact that it does not have the expected symmetry.

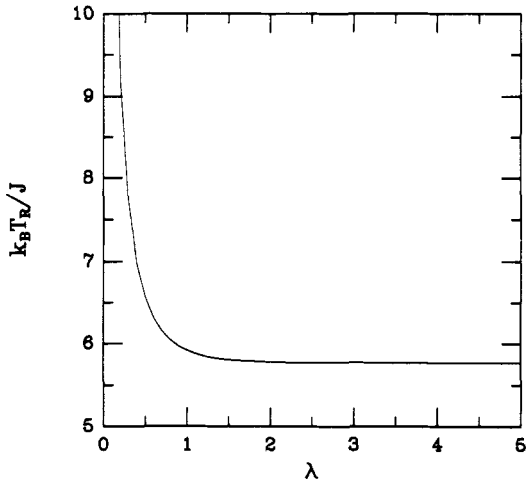

Figure 10. Renormalized roughening temperature for the λ-model. The result is size-independent to numerical accuracy for all values of λ. The phase transition can be interpreted as true roughening for values of $\lambda > 2$ approximately, based on formula (4.4).

5. Concluding remarks

We have carried out an investigation on the general phase diagram structure of a model of roughening for anisotropic surfaces with a preference for a low-temperature reconstructed ground state. The phase diagram, composed of a low-temperature pseudo order–disorder phase transition and a high-temperature roughening transition of possibly variable critical indices, confirms the proposal of Villain and Vilfan (1988) and of Jug and Tosatti (1990) that there should be two separate deconstruction and roughening transitions, for all surfaces having a 1×2 ground state. It is in fact interesting to point out that in a recent x-ray scattering experiment on Pt [110] (Robinson et al 1989) new evidence has been presented for a deconstruction transition at $T_c \sim 1080$ K

† The λ-model thus provides another example besides that of Knops's model (1979), of the *splitting* of the six-vertex roughening into a low-temperature Ising-like disordering plus a very high temperature roughening transition.

leading to a disordered phase with incommensurate correlations (corresponding to a temperature-dependent shift of the diffraction peak). Although it is claimed there that this new phase should also be rough, our results would rather suggest that a separate, higher temperature roughening transition at $T_R > T_c$ should, in principle, exist. Physically the lower transition at T_c corresponds to proliferation of defects in the missing-row structure. It is only at T_R, however, that the defects become unbound. A very similar situation is predicted for Au [110], where $T_c \sim 700$ K (Campuzano *et al* 1985), and for Ir [110].

The present model also predicts two transitions—one of order–disorder character and a roughening transition at a higher temperature—for FCC [110] surfaces which do not reconstruct. The difference between the two temperatures is larger the closer these dormant surfaces are to becoming reconstructed. Precisely at the point where reconstruction sets in ($\kappa = 0$) the disordering temperature appears to vanish, unlike the roughening temperature. It seems possible that the physics of, e.g. Cu [110] (Zeppenfeld *et al* 1989), could be explained by a small negative κ in the present model as a natural extension of the previous description by Trayanov *et al* (1989, 1990) which did not include reconstruction tendencies.

We have proposed, and studied by finite-size transfer-matrix calculations in a simplified version, a statistical model (the λ-model) connecting continuously an Ising-like system with one presenting a six-vertex symmetry. Our results indicate the existence of a phase transition of variable critical exponents, associated with the order–disorder transition in the Ising limit, and drifting towards the non-divergent behaviour in the six-vertex case. Furthermore, the roughening transition, well defined in the six-vertex limit, is shown to be present also for finite values of λ. The temperature remains almost constant for a wide range of λ values, and then rapidly grows towards infinity for $\lambda \rightarrow 0$.

Acknowledgments

One of the authors (GJ) is grateful to MAFF and to the Royal Society for partial support for this work. Helpful discussions with A Levi are also acknowledged. On completion of this work it has come to our attention the close relationship between our results and those of den Nijs (1990) obtained for a different model of the same phenomenon.

References

Alvarado S F, Campagna M, Fattah A and Uelhoff W 1987 *Z. Phys.* B **66** 103

Barber M B 1983 *Phase Transitions and Critical Phenomena* vol 8, ed C Domb and J L Lebowitz (London: Academic)

Baxter R J 1982 *Exactly Solvable Models in Statistical Physics* (London: Academic)

van Beijeren H 1977 *Phys. Rev. Lett.* **38** 993

van Beijeren H and Nolden I 1987 *Structure and Dynamics of Surfaces II* ed W Schommers and P von Blanckenhagen (Berlin: Springer)

Campuzano J C, Foster M S, Jennings G, Willis R F and Unertl W 1985 *Phys. Rev. Lett.* **54** 2684

Cheung H F and McMillan W L 1983 *J. Phys. C: Solid State Phys.* **16** 7027

Domb C 1960 *Adv. Phys.* **9** 149

Drube R, Dose V, Derks H and Heiland W 1989 *Surf. Sci.* **214** L253

Hayden B E, Prince K C, Davie P J, Paolucci G and Bradshaw A M 1983 *Solid State Commun.* **48** 825

Held G A, Jordan-Sweet J L, Horn P M, Mak A and Birgeneau R J 1987 *Phys. Rev. Lett.* **59** 2075
Hetterich W and Heiland W 1989 *Surf. Sci.* **210** 129
Holzer M 1990 *Phys. Rev. Lett.* **64** 653
Jayaprakash C and Saam W F 1984 *Phys. Rev.* B **30** 3916
Jug G and Tosatti E 1990a *Phys. Rev.* B **42** 969
—— 1990b *Physica* A (in press)
Knops H J F 1979 *Phys. Rev.* B **20** 4670
Kohanoff J 1989 *MPhil Thesis* ISAS Trieste unpublished
Kohanoff J, Jug G and Tosatti E 1990 *J. Phys. A: Math. Gen.* **23** L209
Levi A C and Touzani M 1989 *Surf. Sci.* **218** 223
Lieb E H and Wu F Y 1972 *Phase Transitions and Critical Phenomena* vol 1, ed C Domb and M S Green (New York: Academic)
Luck J M 1981 *J. Physique Lett.* **42** L275
Mochrie S G J 1987 *Phys. Rev. Lett.* **59** 304
Nightingale M P 1981 *J. Appl. Phys.* **53** 7927
den Nijs M 1990 *Phys. Rev. Lett.* **64** 435
Onsager L 1944 *Phys. Rev.* **65** 117
Prince K C, Breuer U and Bonzel H P 1988 *Phys. Rev. Lett.* **60** 1146
Robinson I K, Vlieg E and Kern K 1989 *Phys. Rev. Lett.* **63** 2578
Rys F 1963 *Helv. Phys. Acta* **36** 537
Salmerón M and Somorjai G A 1980 *Surf. Sci.* **91** 373
Suzuki M 1974 *Prog. Theor. Phys.* **51** 1992
Trayanov A, Levi A C and Tosatti E 1989 *Europhys. Lett.* **8** 657
—— 1990 *SISSA Preprint* 10 CM; *Surf. Sci.* to be published
Utiyama T 1951 *Prog. Theor. Phys.* **6** 907
Vdovichenko N V 1965 *Sov. Phys. JETP* **21** 350
Villain J and Vilfan I 1988 *Surf. Sci.* **199** 165
Wilkinson J H 1965 *The Algebraic Eigenvalue Problem* (Oxford: Clarendon)
Yang H N, Lu T M and Wang G C 1989 *Phys. Rev. Lett.* **63** 1621
Zeppenfeld P, Kern K, David R and Comsa G 1989 *Phys. Rev. Lett.* **62** 63